

Substrate Activation by Malate Induced by Oxalate in the *Ascaris suum* NAD-Malic Enzyme Reaction[†]

Sang-Hoon Park, Ben G. Harris, and Paul F. Cook*

Appendix: Derivation of the Rate Equation for Substrate Activation by Malate Induced by Oxalate[‡]

Sang-Hoon Park and Paul F. Cook*

Department of Biochemistry and Department of Microbiology and Immunology, Texas College of Osteopathic Medicine, Fort Worth, Texas 76107

Received January 20, 1989; Revised Manuscript Received April 3, 1989

ABSTRACT: Substrate activation of the rate of the NAD-malic enzyme reaction by malate is obtained in the presence but not in the absence of oxalate. The substrate activation is a result of competition between malate and oxalate for the E·NADH complex, with malate binding to the form of the complex unprotonated at an enzyme group with a p*K* of 4.9 and oxalate binding preferentially to the protonated form. The off-rate for NADH from the E·NADH complex is completely rate limiting when the group with a p*K* of 4.9 is protonated but is only one of several rate-limiting steps when it is unprotonated [Kiick, D. M., Harris, B. G., & Cook, P. F. (1986) *Biochemistry* 25, 227]. The competition by malate with oxalate thus results in an overall increase in the off-rate for NADH as a result of binding to the unprotonated form of E·NADH. Consistent with the proposed mechanism, the deuterium isotope effect on *V* for the nonsubstrate-activating malate concentration range decreases from 1.6 in the absence of oxalate to 1.3 in the presence of a concentration of oxalate equal to its *K*_{ij}. The rate equation for the oxalate-induced substrate activation by malate is derived and presented in the Appendix. Data are discussed in terms of the overall mechanism of the NAD-malic enzyme.

The NAD-malic enzyme from *Ascaris suum* has been shown to have a steady-state random mechanism in which Mg²⁺ must bind prior to malate for productive quaternary E·NAD·Mg²⁺·malate complex formation (Park et al., 1984). The above mechanism was confirmed and the existence of the E·NAD·malate and E·malate complexes was documented by Kiick et al. (1984), who used protection against thiol modification by 5,5'-dithiobis(2-nitrobenzoate) to determine the dissociation constants for a number of enzyme-reactant complexes.

More recently, Kiick et al. (1986) showed using initial velocity studies, pH studies, and deuterium isotope effects that release of NADH is slow. The off-rate for NADH is pH dependent, becoming slower at pH values below 7 until at pH 4 it completely limits the overall reaction. This slow down in the off-rate for NADH occurs upon protonation of an enzyme residue with a p*K* of 4.9 responsible for accepting the proton from the 2-hydroxyl group of L-malate during the hydride transfer step. Inhibition by oxalate is competitive vs malate at pH 7 and above but noncompetitive vs malate at pH values below 7. The intercept inhibition was shown to be a result

of binding of oxalate to the E·NADH complex by double-inhibition studies with NADH and oxalate. In addition, oxalate binds with much higher affinity to enzyme in which the group with a p*K* of 4.9 is protonated.

Although binding of oxalate to E·NADH was documented, substrate inhibition by malate was not observed. If malate does bind to the E·NADH complex, it apparently has no effect on the off-rate for NADH, a possibility also suggested by Schimerlik and Cleland (1977) for the cytoplasmic NADP-malic enzyme from pigeon liver. In the present study, it is shown that L-malate does bind to the E·NADH complex and that it does not affect the off-rate for NADH. In addition, oxalate induces substrate activation by malate as a result of the competition of oxalate for the E·NADH complex protonated at the general base and malate for the unprotonated form of this binary complex.

MATERIALS AND METHODS

Enzymes. Mitochondrial NAD-malic enzyme from *Ascaris suum* was purified according to the procedure of Allen and Harris (1981). Enzyme was homogeneous by the criterion of sodium dodecyl sulfate (SDS)¹-polyacrylamide gel electrophoresis run according to the method of O'Farrell (1975) as modified by Atkins et al. (1975). Enzyme had a final specific activity of 35 units/mg assayed in the direction of oxidative decarboxylation using 100 mM Hepes,¹ pH 7.5, 1.0 mM DTT, 310 mM L-malate (24 mM when corrected for Mg-malate), 32.8 mM NAD (2 mM when corrected for Mg-NAD), and 618 mM MgSO₄ (300 mM when corrected for Mg-malate and Mg-NAD). The enzyme was stored as described previously by Allen and Harris (1981).

[†] This work was supported by National Institutes of Health Grants AI 24155 (to B.G.H.) and GM 36799 (to P.F.C.), by Robert A. Welch Foundation Grants B-997 (to B.G.H.) and B-1031 (to P.F.C.), by Grant BRSG SO7 RR07195 awarded by the Biomedical Research Grant Program (to P.F.C.), Division of Research Resources, National Institutes of Health, and by a Faculty Research Grant from the University of North Texas (to P.F.C.).

* Address correspondence to this author at the Department of Microbiology and Immunology, Texas College of Osteopathic Medicine.

[‡] This work was supported by National Institutes of Health Grant GM 36799 (to P.F.C.), by Robert A. Welch Foundation Grant B-1031, by Grant BRSG SO7 RR07195 awarded by the Biomedical Research Grant Program, Division of Research Resources, National Institutes of Health, and by a Faculty Research Grant from the University of North Texas. P.F.C. was the holder of an NIH Research Career Development Award during the time this work was completed (AM01155).

¹ Abbreviations: DTT, dithiothreitol; EDTA, ethylenediaminetetraacetic acid; Hepes, *N*-(2-hydroxyethyl)piperazine-*N'*-2-ethanesulfonic acid; Mes, 2-(*N*-morpholino)ethanesulfonic acid; SDS, sodium dodecyl sulfate.

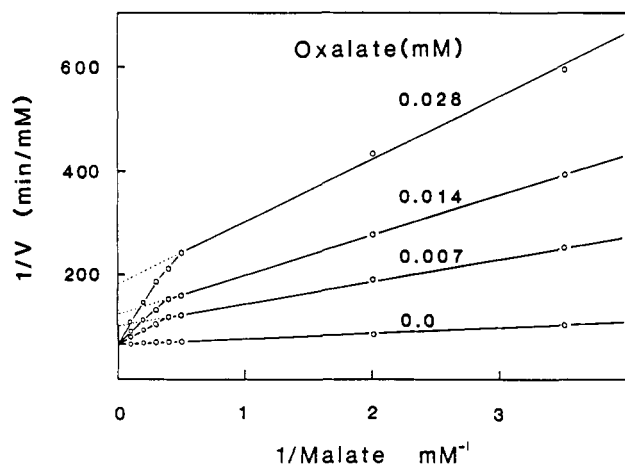


FIGURE 1: Initial velocity pattern obtained by varying [malate] at different fixed levels of [oxalate]. Conditions are as follows: 100 mM Mes, pH 5.4, 2 mM NAD, and 80 mM MnSO₄. The concentrations of malate and oxalate were varied as shown. Data for the high 1/[malate] asymptote (called the NC_{asym}) were fitted by using eq 2 while the low 1/[malate] asymptote (called the C_{asym}) data were fitted by using eq 1. Points are experimental while solid lines are theoretically based on the fitted parameters.

Chemicals. The dinucleotide NAD was from Boehringer-Mannheim. L-Malate, DTT, 1,4-bis(hydroxyethyl)piperazine, Mes, Hepes, EDTA, maleate, triethanolamine, and glycerol were from Sigma. MnSO₄, MgSO₄, and oxalate were from Fisher. The concentration of NAD was determined spectrophotometrically by using an extinction coefficient of 17 800 M⁻¹ cm⁻¹ at 259 nm. All other chemicals and reagents were obtained from commercial sources and were of the highest purity available.

Preparation of L-Malate-2-d. L-Malate-2-d was prepared enzymatically by using a modification of the procedure of Viola and Cook (1979). The difference from the previously published procedure is that all reactant concentrations were tripled and the protein precipitant HClO₄ was replaced by H₂SO₄ to prevent cracking in the AG1 × 8 column and to prevent inhibition of the malic enzyme reaction by ClO₄⁻. According to the modified procedure, addition of H₂SO₄ should be very slow since localized high concentrations of H₂SO₄ tend to redissolve the protein precipitate.

Initial Velocity Studies. All assays were carried out at 25 °C with a Gilford 2600 spectrophotometer connected to a Hewlett-Packard 7225B graphics plotter and a Gilford thermal printer. The temperature was maintained with a circulating water bath with the capacity to heat and cool the thermospacers of the Gilford 2600. Reaction cuvettes were 1 cm in path length and 1 mL in volume. All cuvettes were incubated for at least 10 min in the water bath prior to assay. A typical assay contained 100 mM buffers [1,4-bis(hydroxyethyl)piperazine (pH 4.5–5.5), Mes (pH 5.5–6.5), or Hepes (pH 6.5–7.3)], 1 mM DTT, 80 mM Mn²⁺ (or 140 mM Mg²⁺), 2 mM NAD, 0.2–10 mM L-malate, and 16 nM malic enzyme. All assays reflected initial velocity conditions with less than 10% of the limiting reactant utilized over the time course of the reaction. For pH studies, all assays were duplicates with points shown as the average of the duplicate values. The standard error is within the size of the point. The pH is measured to ±0.01 pH unit, and in all cases, negligible pH changes were observed before and after reaction. Since total substrate and inhibitor concentrations were sometimes high, substrate and inhibitor stock solutions were titrated to the approximate pH value of the assay.

Metal Chelate Correction. The concentrations of malate, NAD, oxalate, and metal ions discussed above were corrected

for the concentration of metal-ligand chelate complexes according to Park et al. (1984). Dissociation constants used in the above corrections are as follows: Mg-NAD, 19.5 mM; Mg-malate, 25.1 mM; Mg-oxalate, 1.7 mM; Mg-(oxalate)₂, 58 mM²; Mn-NAD, 6.3 mM; Mn-malate, 12.9 mM; Mn-oxalate, 0.6 mM; Mn-(oxalate)₂, 40 mM². All other reaction components gave negligible corrections for the concentration conditions used.

Data Processing. Reciprocal initial velocities were plotted vs reciprocal substrate concentrations. Data were fitted with the appropriate rate equations and computer programs developed by Cleland (1979). Data for competitive and non-competitive inhibition were fitted by using

$$v = VA/[K_a(1 + I/K_{is}) + A] \quad (1)$$

$$v = VA/[K_a(1 + I/K_{is}) + A(1 + I/K_{ii})] \quad (2)$$

Data for pK_{is} profiles for oxalate were fitted with eq 3 while pK_{ii} profiles were fitted with eq 4, and data for deuterium isotope effects were fitted with eq 5. In eq 1, 2, and 5, A and

$$\log y = \log [Y_L + Y_H(K_1/K)/(1 + K_1/H)] \quad (3)$$

$$\log y = \log [C/(1 + K_1/H)] \quad (4)$$

$$v = VA/[K_a(1 + F_i E_{V/K}) + A(1 + F_i E_V)] \quad (5)$$

I are reactant and inhibitor concentrations, respectively, K_a is the Michaelis constant for A , K_{is} and K_{ii} are inhibition constants for the slope and intercept, respectively, V is the maximum velocity, v is the observed initial velocity, F_i is the fraction of deuterium in L-malate-2-d, and $E_{V/K}$ and E_V are isotope effects minus 1 for the two parameters V/K and V , respectively. In eq 3 and 4, Y_L and Y_H are the low- and high-pH constant values of $1/K_{is}$, K_1 is the dissociation constant for an enzyme residue, C is the pH-independent value of $1/K_{ii}$, and y is the observed value of $1/K_{is}$ or $1/K_{ii}$ at any pH.

RESULTS AND DISCUSSION

It has been shown previously (Kiick et al., 1986) that oxalate inhibits competitively vs malate at pH values of 6.5 and above with Mg²⁺ as the divalent metal ion activator. At low pH, the inhibition becomes noncompetitive. The switch from competitive inhibition at pH values above 6.5 to noncompetitive inhibition at pH values of 6.5 and below was shown to be a result of decreasing the off-rate of NADH at low pH, allowing sufficient E·NADH·Mg to build up in the steady state. Oxalate was then able to bind to both E·NAD·Mg and E·NADH·Mg to give net noncompetitive inhibition (Kiick et al., 1986). This was confirmed by using double inhibition by NADH and oxalate vs malate. The latter studies were carried out using malate concentrations of 0.5–5 mM. With Mn²⁺ as the divalent metal ion activator, inhibition by oxalate is noncompetitive over the pH range 4.5–7 (data not shown).

The saturation curve for L-malate obtained in the absence of products and dead-end inhibitors at saturating levels of NAD and Mn²⁺ gives a linear double-reciprocal plot over the range 0.3–10 mM L-malate. In the presence of oxalate, however, double-reciprocal plots are concave downward (Figure 1). Thus, substrate activation by malate is obtained in the presence but not in the absence of oxalate. This substrate activation is obtained as a result of malate competing with oxalate for the E·NADH·Mn²⁺ complex, relieving the inhibition by oxalate. The competition for product complex by malate and oxalate is not a simple one. The NAD-malic enzyme catalyzes its reaction via general acid and general base

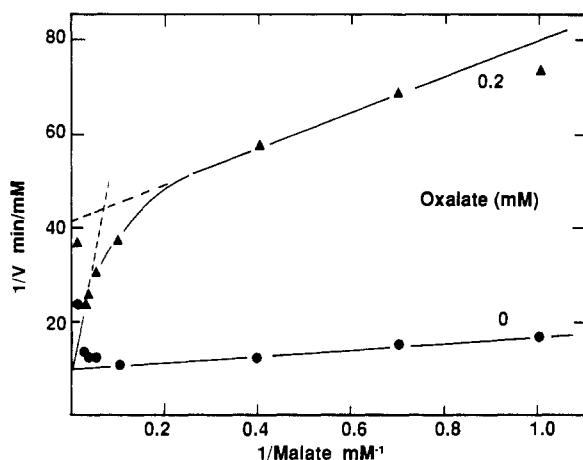


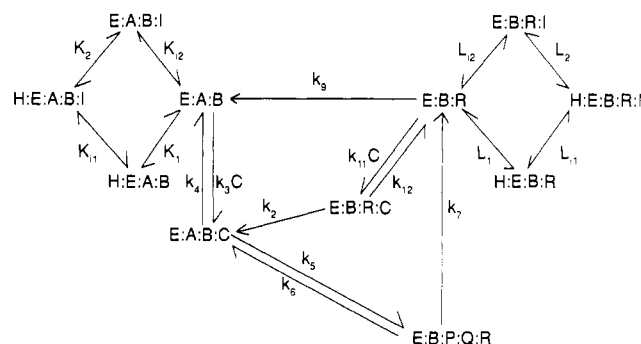
FIGURE 2: Initial velocity data obtained by varying [malate] in the presence of oxalate. Conditions are as follows: 100 mM Mes, pH 5.9, 2 mM NAD, and 150 mM MgSO_4 . The concentrations of malate and oxalate are as shown. Points are experimental while solid lines are drawn by eye.

catalysis. The general base has a pK of 4.9 and accepts the C-2 hydroxyl proton concomitant with hydride transfer. The general acid has a pK of 9 and is thought to donate a proton to the enol of pyruvate to facilitate the tautomerization to pyruvate. Oxalate has been shown to preferentially bind to enzyme protonated at the general base by about 2 orders of magnitude compared to enzyme unprotonated at this group. Malate, on the other hand, binds to enzyme only when the general base is unprotonated and the general acid is protonated. As a result, malate is expected to bind to the $\text{E}\cdot\text{NADH}\cdot\text{Mn}^{2+}$ complex while oxalate prefers binding to the $\text{H}\cdot\text{E}\cdot\text{NADH}\cdot\text{Mn}^{2+}$ complex. In addition, since no substrate activation is observed by malate in the absence of oxalate, the binding of malate to $\text{E}\cdot\text{NADH}\cdot\text{Mn}^{2+}$ does not affect the off-rate for NADH. A repeat of the experiment shown in Figure 1 with Mg^{2+} as the divalent metal ion activator gives qualitatively similar results when malate is varied over a wider concentration range (0.5–40 mM) than that used previously (0.5–5 mM; Kiick et al., 1986) (Figure 2). The plots with Mg^{2+} are further complicated, however, since there is a decrease in rate above 40 mM uncomplexed malate as a result of the high ionic strength.

A model consistent with the above is shown in Scheme I. The rate equation in double-reciprocal form based on Scheme I is given in eq A1 of the Appendix accompanying this paper. In Scheme I, A, B, C, P, Q, R, H, and I are NAD, M^{2+} , malate, CO_2 , pyruvate, NADH, H^+ , and oxalate, respectively. The rate constants k_3 and k_{11} represent the addition of malate to $\text{E}\cdot\text{NAD}\cdot\text{M}^{2+}$ and $\text{E}\cdot\text{NADH}\cdot\text{M}^{2+}$, respectively, while k_4 and k_{12} represent release of malate from $\text{E}\cdot\text{NAD}\cdot\text{M}\cdot\text{malate}$ and $\text{E}\cdot\text{NADH}\cdot\text{M}\cdot\text{malate}$, respectively. The rate constants k_5 and k_6 represent interconversion of the central substrate and product complexes; k_7 represents the release of CO_2 and pyruvate; k_9 and k_2 represent release of NADH from $\text{E}\cdot\text{NADH}\cdot\text{M}^{2+}$ and $\text{E}\cdot\text{NADH}\cdot\text{M}\cdot\text{malate}$, respectively. The constants K_1 and K_2 represent acid dissociation constants for the $\text{H}\cdot\text{E}\cdot\text{NAD}\cdot\text{M}^{2+}$ and $\text{H}\cdot\text{E}\cdot\text{NAD}\cdot\text{M}\cdot\text{oxalate}$ complexes, respectively, while L_1 and L_2 represent acid dissociation constants for $\text{H}\cdot\text{E}\cdot\text{NADH}\cdot\text{M}^{2+}$ and $\text{H}\cdot\text{E}\cdot\text{NADH}\cdot\text{M}\cdot\text{oxalate}$, respectively. The constants K_{11} and K_{12} represent dissociation constants for oxalate from $\text{H}\cdot\text{E}\cdot\text{NAD}\cdot\text{M}\cdot\text{oxalate}$ and $\text{E}\cdot\text{NAD}\cdot\text{M}\cdot\text{oxalate}$ complexes, respectively, while L_{11} and L_{12} are dissociation constants for oxalate from $\text{H}\cdot\text{E}\cdot\text{NADH}\cdot\text{M}\cdot\text{oxalate}$ and $\text{E}\cdot\text{NADH}\cdot\text{M}\cdot\text{oxalate}$ complexes, respectively.

A plot of eq A1 from the Appendix as E_i/v vs $1/C$ is concave downward (see Figure 4 in the Appendix), consistent with

Scheme I: Mechanism for Substrate Activation by C in the Presence of I^a



^a C and I compete for the sum of EBR and HEBR. The thermodynamic box containing EAB, HEAB, EABI, and HEABI is a rapid equilibrium segment called X, while the thermodynamic box containing EBR, HEBR, EBR I, and HEBR I is a rapid equilibrium segment called Y.

the data shown in Figures 1 and 2. This plot has asymptotes at high values of $1/C$ (called the noncompetitive asymptote and denoted NC_{asym}) and at values of $1/C$ near zero (called the competitive asymptote and denoted C_{asym}). The extrapolated asymptotes cross at a single point (see Figure 4 in the Appendix). The equation (Appendix eq A12) for the x coordinate of the crossover point for the competitive and noncompetitive asymptotes provides information on the affinity of malate for the $\text{E}\cdot\text{NADH}$ complex (actually most likely the $\text{E}\cdot\text{NADH}\cdot\text{M}^{2+}$ complex since the divalent metal ion concentration is saturating). The expression for the x coordinate from Appendix eq A12 is $k_{11}k_2/(k_2 + k_{12})k_9$, the ratio of the net off-rates for NADH under conditions where the malate concentration is high enough to give apparent substrate activation [$k_2k_{11}/(k_2 + k_{12})$] to the off-rate where the malate concentration is not high enough to give substrate activation (k_9).

In the absence of the inhibitor, oxalate, the rate constants k_2 and k_9 must be equal since the double-reciprocal plot is linear under these conditions even when malate should be saturating for binding to the $\text{E}\cdot\text{NADH}\cdot\text{M}^{2+}$ complex.² From previous work making use of primary deuterium isotope effects (Kiick et al., 1986) and isotope partitioning studies (Chen et al., 1988) with Mg^{2+} as the divalent metal ion, it is known that k_4 and k_9 are equal. In addition, k_3 is probably also equal to k_{11} since these rate constants represent the binding of malate to two very similar complexes, $\text{E}\cdot\text{NAD}\cdot\text{M}^{2+}$ and $\text{E}\cdot\text{NADH}\cdot\text{M}^{2+}$. The similarity of the two complexes is shown by the equality of k_4 and k_9 , the identity of the dissociation constants for the $\text{H}\cdot\text{E}\cdot\text{NAD}\cdot\text{M}\cdot\text{oxalate}$ (K_{11}) and the $\text{H}\cdot\text{E}\cdot\text{NADH}\cdot\text{M}\cdot\text{oxalate}$ (L_{11}) complexes (discussed below), and the values for K_i for $\text{E}\cdot\text{NAD}\cdot\text{M}^{2+}$ (30 μM ; Park et al., 1984) and for $\text{E}\cdot\text{NADH}\cdot\text{M}^{2+}$ (50 μM ; unpublished work of Sushanta Mallick in this laboratory). Since oxalate is an inhibitor competitive with malate and oxalate binds with equal affinity to $\text{H}\cdot\text{E}\cdot\text{NAD}\cdot\text{M}^{2+}$ and $\text{H}\cdot\text{E}\cdot\text{NADH}\cdot\text{M}^{2+}$ complexes, these complexes must be very similar. The rates of dissociation of malate and NADH are slow steps compared to the catalytic interconversion steps (Kiick et al., 1986). With $k_2 = k_9$, the expression

² Experimental data indicate that C_{asym} is identical with NC_{asym} at $[I] = 0$. From the equality of the intercepts (from eq A9 and A11 in the Appendix) when $[I] = 0$, substituting for f_3 and f_9 gives $1/k_2 = (1 + [H]/L_1)/k_9 - k_2k_{11}/(k_3k_9(k_2 + k_{12}))$. This expression holds at all pH values so that $1/k_2$ is also equal to $1/k_9 - k_2k_{11}/[k_3k_9(k_2 + k_{12})]$. The same V is attained at infinite [malate], indicating that k_2 must equal k_9 and thus $k_2k_{11}/[k_3k_9(k_2 + k_{12})]$ must be near zero. Since the expression can be reduced to $k_{11}/[k_3(k_2 + k_{12})]$ and it is known (see text) that $k_{11}/(k_2 + k_{12})$ approximates $1/K_4$ for the $\text{E}\cdot\text{NADH}\cdot\text{M}^{2+}$ complex (K_4 values of 2 and 15 mM are obtained with Mn^{2+} and Mg^{2+} , respectively), it is likely the value for k_3 sets the expression near zero.

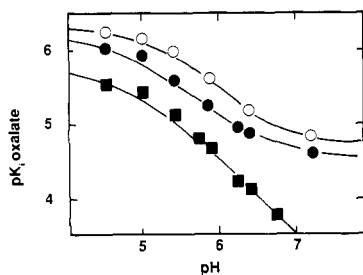


FIGURE 3: pH dependence of $1/K_i$ for oxalate. The upper two curves are for the slope inhibition constant obtained from inhibition in the competitive and noncompetitive asymptotic regions, respectively, while the bottom curve is for $1/K_{ii}$ from the noncompetitive asymptotic region. Conditions are given under Materials and Methods. Points are experimental while curves are from fits using eq 3 and 4.

for the x coordinate reduces to $k_{11}/(k_2 + k_{12})$. Since the value for $(k_{12} + k_2)/k_{11}$ is 2 mM, greater than the value for k_4/k_3 (0.2 mM), and since $k_4 = k_2$ [with Mg^{2+} but $k_4 > k_2$ with Mn^{2+} since the value for $^D V(1.6) < ^D(V/K_{\text{malate}})(2.2)$] and $k_3 = k_{11}$, k_{12} must be greater than k_2 , and the x coordinate of the crossover point must be the reciprocal of the dissociation constant for the E·NADH·Mn-malate complex. In the case of Mg^{2+} , the dissociation constant is approximately 15 mM.

The pH dependence of the dissociation constant for oxalate with Mn^{2+} as the divalent metal ion activator can be obtained for both asymptotes. In the case where the malate concentration is low, the inhibition by oxalate is noncompetitive as can be seen in Figure 1 for the extrapolated asymptotes. The $\text{app}K_{is}$ under these conditions is for the E·NAD·Mn-oxalate complex while the $\text{app}K_{ii}$ is for the E·NADH·Mn-oxalate complex (Kiick et al., 1986). In both cases, $1/K_i$ is constant at low pH and in the case of K_{is} decreases to a new constant value at high pH (Figure 3). This was also shown to be true for data previously obtained with Mg^{2+} as the divalent metal ion activator (Kiick et al., 1986). In Figure 3, the curve with the closed circles represents the pH dependence of $\log(1/\text{app}K_{is})$ obtained from a plot of the slopes of the noncompetitive asymptotes vs [oxalate], that is, from the slopes of asymptotes at high $1/[\text{malate}]$ such as those shown in Figure 1 as a function of [oxalate]. Theoretically, the $\text{app}K_{is}$ is described by the rapid equilibrium segment given as X in Scheme I. The equation for the pH dependence of $\text{app}K_{is}$ is given by eq A15 in the Appendix. The low pH constant value is K_{i1} while the high pH constant value is K_{i2} where K_{i1} is less than K_{i2} in the present case. The values of K_{i1} , K_{i2} , $\text{p}K_1$, and $\text{p}K_2$ obtained from a fit of eq 3 to the data are $0.50 \pm 0.03 \mu\text{M}$, $20.1 \pm 0.1 \mu\text{M}$, 5.3 ± 0.2 , and 6.8 ± 0.1 , respectively. The curve with the closed squares in Figure 3 represents the pH dependence of $1/\text{app}K_{ii}$ obtained from the extrapolated ordinate intercepts of the noncompetitive asymptotes as a function of [oxalate], e.g., the dotted lines shown in Figure 1. Theoretically, the $\text{app}K_{ii}$ is described by the rapid equilibrium segment given as Y in Scheme I. The equation for the pH dependence of $\text{app}K_{ii}$ is given by eq A18 in the Appendix. As noted in the Appendix (eq A19), only if $L_{i1} = K_{i1}$ will the low pH constant value be equal to L_{i1} . The experimentally determined value of the low pH constant value of K_{ii} is $3.0 \pm 0.2 \mu\text{M}$, 6-fold higher than the value of $0.5 \mu\text{M}$ obtained for K_{i1} . However, this difference partially reflects the fact that since release of NADH from E·NADH·Mn $^{2+}$ does not completely limit the overall reaction (Kiick et al., 1986; Chen et al., 1988), not all of the enzyme piles up as E·NADH·Mn $^{2+}$ in the steady state at saturating concentrations of NAD, Mn $^{2+}$, and malate. It will be shown below that in fact $K_{i1} = L_{i1}$. The curve with the open circles in Figure 3 represents the pH dependence of $\log(1/\text{app}K_{is})$ obtained from a plot of the slopes of the competitive asymptotes vs [oxalate], that is, from the slopes of asymptotes at low

$1/[\text{malate}]$ such as those shown in Figure 1 as a function of [oxalate]. Theoretically, the $\text{app}K_{is}$ is described by the rapid equilibrium segment given as Y in Scheme I. The equation for the pH dependence of $\text{app}K_{is}$ is given by eq A22 in the Appendix. There is a difference between the $\text{app}K_{ii}$ obtained from the extrapolated asymptotes of the noncompetitive region and the $\text{app}K_{is}$ obtained from the competitive asymptote. In the latter case, the K_i is directly measured from competition between oxalate and malate and does not therefore depend on the amount of the E·NADH·Mn $^{2+}$ complex present. As seen in eq A22, however, the two cases ($\text{app}K_{ii}$ for NC_{asym} and $\text{app}K_{is}$ for C_{asym}) are similar in that the low pH constant value will be L_{i1} if L_{i1} is equal to K_{i1} . The pH-independent value of K_{is} at low pH is $0.43 \pm 0.06 \mu\text{M}$, identical with the value of K_{i1} and suggesting that $L_{i1} = K_{i1}$. The difference in low pH independent values for K_{i1} and the $\text{app}K_{ii}$ allows an estimate of the amount of enzyme that exists in the steady state under conditions where NAD, Mn $^{2+}$, and malate are saturating. The slowest step under these conditions is decarboxylation as judged by the ^{13}C isotope effect on decarboxylation³ with NADH release from the E·NADH·Mn $^{2+}$ complex also contributing to the rate limitation. Since the $\text{app}K_{ii}$ is about 6-fold less than the value of L_{i1} , only 17% of the enzyme is E·NADH·Mn $^{2+}$ in the steady state with the remainder present as central complexes.

In addition to the K_i for oxalate, the $\text{p}K$ for the enzyme group protonated for optimum oxalate binding is the same (at least within experimental error) whether the E·NAD·Mn $^{2+}$ or E·NADH·Mn $^{2+}$ complex is titrated. This is based on the equality in the $\text{p}K$ obtained in V and V/K_{malate} pH profiles, as well as the $\text{p}K$ obtained from the pH dependence of the deuterium isotope effect on V (Kiick et al., 1986). The $\text{p}K$ value obtained for the E·NAD·Mn $^{2+}$ complex ($\text{p}K_{is}$ from NC_{asym}) is 4.9 ± 0.1 while that obtained for the E·NADH·Mn $^{2+}$ complex ($\text{p}K_{ii}$ from NC_{asym} and $\text{p}K_{is}$ from C_{asym}) is 4.9 ± 0.1 . The $\text{p}K$ value obtained for E·NAD·Mn-oxalate ($\text{p}K_{is}$ from NC_{asym}) is 6.5 ± 0.1 , while that obtained for E·NADH·Mn-oxalate ($\text{p}K_{is}$ from C_{asym}) is 6.6 ± 0.1 . These data are identical with those obtained by Kiick et al. (1986) using Mg^{2+} as the divalent metal ion. The identity of $\text{p}K$ values obtained for the same enzyme base in oxidized and reduced dinucleotide complexes further attests to the similarity of these two complexes.

If the mechanism depicted in Scheme I and the derived rate equation accurately reflects the behavior observed experimentally, the ratio of the experimentally determined K_i values at any two pH values should be calculable from eq A15. For example, at pH 7.2, the $\text{app}K_{is}$ from the NC_{asym} (closed circles, Figure 3) is $25 \mu\text{M}$ while at pH 5 it is $1.2 \mu\text{M}$. The experimental ratio is 20.8. The ratio calculated from eq A15 using values of 4.9 for $\text{p}K_1$ and 6.7 for $\text{p}K_2$ and pH values of 7.2 and 5 is $47.8/2.2$ or 21.7, in excellent agreement with the experimentally obtained ratio. This excellent agreement holds for ratios calculated at any two pHs using data obtained for $\text{p}K_{is}$ profiles.

Another test of the proposed mechanism is the behavior of the deuterium isotope effects. If oxalate binding to the H·E·NADH·Mn $^{2+}$ complex does result in a decrease in the off-rate for NADH, the value for $^D V$ (V for the extrapolated NC_{asym}) should decrease with respect to that obtained in the

³ The value for $^{13}(V/K_{\text{malate}})$ is 1.035 ± 0.001 (unpublished results of Dr. Paul M. Weiss of the University of Wisconsin—Madison). The ^{13}C effect is a V/K effect, but it is known that the off-rates for reactants from E·NAD·Mn-malate are equal to the off-rate for NADH from E·NADH·Mn $^{2+}$ and that the deuterium isotope effects on V and V/K_{malate} are equal so that the ^{13}C effect under V conditions should be identical with that obtained under V/K conditions.

absence of oxalate. In the absence of oxalate, values of 2.2 and 1.6 are obtained for $^D(V/K_{\text{malate}})$ and DV , respectively, with Mn^{2+} as the divalent metal ion (Gavva, 1988). Deuterium isotope effects in the presence of 5 μM oxalate at pH 5.5 measured for the noncompetitive region with Mn^{2+} as the divalent metal ion are $^D(V/K_{\text{malate}}) = 2.4 \pm 0.3$ and $^DV = 1.35 \pm 0.05$. The isotope effect on V/K_{malate} is identical with that obtained at zero oxalate while the isotope effect on V is lower than the value of 1.6 as predicted by the mechanism shown in Scheme I. The decreased effect on V indicates a slowing down of a step other than hydride transfer and after release of the first product (likely to be CO_2) since the value of $^D(V/K_{\text{malate}})$ does not change. This step is almost certainly NADH release.

The deuterium isotope effect of 1.6 on V is the value obtained at infinite malate concentration including the substrate activation region. The value of $^D(V/K_{\text{malate}})$ obtained for the C_{asym} region, however, is 1.34 ± 0.10 , much lower than the value obtained for $^D(V/K_{\text{malate}})$ for the noncompetitive region. The lower value is expected from a consideration of the expressions for C_f derived for the competitive (eq A25) and noncompetitive (eq A28, where C_f is k_5/k_4) regions of the curve. Since data were collected at pH 5.5, the first term in the numerator of eq A25 will not increase C_f substantially. The $1 + H/K_1$ term is calculated to be only 0.25 while the I/L_{11} and I/L_{12} terms are estimated at 10 and 0.25, respectively, assuming L_{11} and L_{12} are equal to K_{11} and K_{12} , a reasonable assumption as shown above. It is the contribution of the induced substrate activation pathway that contributes most to the increase in C_f at this pH. This is expected since the V/K for the substrate activation region is not really a V/K in the true sense, i.e., the rate under conditions where malate is limiting for the overall reaction and all other reactants are saturating. It is instead an apparent V/K for substrate activation obtained under conditions in which the addition of malate to the $\text{E} \cdot \text{NADH} \cdot \text{Mn}^{2+}$ complex is limiting, i.e., V_{max} conditions.

Thus, the data are qualitatively and quantitatively consistent with a mechanism in which malate and oxalate bind optimally to forms of the $\text{E} \cdot \text{NADH} \cdot \text{Mn}$ complex unprotonated and protonated, respectively, at a general base with a pK of 4.9. Protonation of this general base has been shown (Kiick et al., 1986) to result in a decrease in the off-rate for NADH with oxalate stabilizing the protonated form. Malate binds to the unprotonated form of the complex so that at infinite malate concentration the unprotonated form is stabilized. The off-rate for NADH is not affected by bound malate, and thus when the malate concentration is very high in the presence of oxalate, the off-rate for NADH is effectively increased as a result of a shift in the equilibrium between unprotonated and protonated forms of the $\text{E} \cdot \text{NADH} \cdot \text{Mn}$ complex. The result is substrate activation by malate.

Registry No. NAD-malic enzyme, 9028-46-0; malate, 97-67-6; deuterium, 7782-39-0; oxalate, 144-62-7; L-malate-2-d, 71655-88-4.

REFERENCES

- Allen, B. L., & Harris, B. G. (1981) *Mol. Biochem. Parasitol.* 2, 367.
- Atkins, J. F., Lewis, J. B., Anderson, C. W., & Testelend, R. (1975) *J. Biol. Chem.* 250, 5688.
- Chen, C.-Y., Harris, B. G., & Cook, P. F. (1988) *Biochemistry* 27, 212.
- Cleland, W. W. (1979) *Methods Enzymol.* 63, 103.
- Gavva, S. R. (1988) Ph.D. Dissertation, University of North Texas, Denton, TX.
- Kiick, D. M., Allen, B. L., Rao, J. G. S., Harris, B. G., & Cook, P. F. (1984) *Biochemistry* 23, 5454.
- Kiick, D. M., Harris, B. G., & Cook, P. F. (1986) *Biochemistry* 25, 227.
- O'Farrell, D. H. (1975) *J. Biol. Chem.* 250, 4007.
- Park, S.-H., Kiick, D. M., Harris, B. G., & Cook, P. F. (1984) *Biochemistry* 23, 5446.
- Schimerlik, M. I., & Cleland, W. W. (1977) *Biochemistry* 16, 565.
- Viola, R. E., Cook, P. F., & Cleland, W. W. (1979) *Anal. Biochem.* 96, 334.

APPENDIX: DERIVATION OF THE RATE EQUATION FOR SUBSTRATE ACTIVATION BY MALATE INDUCED BY OXALATE

Under conditions in which NAD and Mn^{2+} (or Mg^{2+}) are saturating and malate is varied at different fixed levels of oxalate, the mechanism depicted in Scheme I applies where A, B, C, P, Q, R, and I are NAD, Mn^{2+} (or Mg^{2+}), L-malate, pyruvate, CO_2 , NADH, and oxalate, respectively. The segments X and Y are assumed to be in rapid equilibrium. An equation based on a mechanism similar to that given above was derived previously by Dalziel and Dickinson (1966) to describe the substrate activation observed by cyclohexanol in the equine liver alcohol dehydrogenase reaction. The difference between the two treatments is that the present mechanism allows for inhibitor binding and also for different protonation states of enzyme-reactant (or inhibitor) complexes.

Using the method of King and Altman (1956) and applying the rapid equilibrium assumption of Cha (1968) to segments X and Y, we derived the rate equation describing Scheme I:

$$[E_t]/v = \{f_9k_9(k_2 + k_{12})(k_4k_6 + k_4k_7 + k_5k_7)/[C]^2 + [f_3k_3(k_5k_7 + f_9k_5k_9 + f_9k_6k_9 + f_9k_7k_9)(k_2 + k_{12}) + f_{11}k_2k_4k_{11}(k_6 + k_7)]/[C] + f_3f_{11}k_3k_{11}(k_2k_5 + k_2k_6 + k_2k_7 + k_5k_7)\}/\{f_3f_9k_3k_5k_7k_9(k_2 + k_{12})/[C] + f_3f_{11}k_2k_3k_5k_7k_{11}\} \quad (\text{A1})$$

where f_3 , f_9 , and f_{11} are defined as

$$f_3 = \frac{1}{1 + [I]/K_{12} + [H]/K_1 + [H][I]/K_1K_{11}} \quad (\text{A2})$$

$$f_9 = f_{11} = \frac{1}{1 + [I]/L_{12} + [H]/L_1 + [H][I]/L_1L_{11}} \quad (\text{A3})$$

Equation A1 can be rewritten generally as

$$\frac{[E_t]}{v} = \frac{DZ^2 + EZ + F}{GZ + H} \quad (\text{A4})$$

where $Z = 1/C$ and the coefficients D , E , F , G , and H are $f_9k_9(k_2 + k_{12})(k_4k_6 + k_4k_7 + k_5k_7)$, $f_3k_3(k_5k_7 + f_9k_5k_9 + f_9k_6k_9 + f_9k_7k_9)(k_2 + k_{12}) + f_{11}k_2k_4k_{11}(k_6 + k_7)$, $f_3f_{11}k_3k_{11}(k_2k_5 + k_2k_6 + k_2k_7 + k_5k_7)$, $f_3f_9k_3k_5k_7k_9(k_2 + k_{12})$, and $f_3f_{11}k_2k_3k_5k_7k_{11}$, respectively. Equation A4 describes a function such as that shown in Figure 4. For Figure 4, two asymptotes can be defined, one at high values of $1/C$ (C_{asym}) and a second at $1/C$ near zero (C_{asym}). Equations for the C asymptotes can be obtained by differentiating $[E_t]/V$ with respect to $1/C$, giving

$$\frac{d([E_t]/V)}{dZ} = \frac{DGZ^2 + 2DZH + (EH - FG)}{G^2Z^2 + 2GHZ + H^2} \quad (\text{A5})$$

The slope of C_{asym} is obtained at $Z = 0$ and is given as

$$\text{slope of } C_{\text{asym}} = (E/H) - (FG/H^2) \quad (\text{A6})$$

Substituting the expressions for E , F , G , and H gives

$$\text{slope of } C_{\text{asym}} = k_4(k_6 + k_7)/f_3k_3k_5k_7 + (k_2 + k_{12})/k_2k_{11}f_{11} - k_9(k_2 + k_{12})/k_2^2k_{11} \quad (\text{A7})$$